

# State-to-State Dynamics of the $\text{H} + \text{CDCl}_3(v_1''=1) \rightarrow \text{HD}(v',j') + \text{CCl}_3$ Reaction

Dominick V. Lanzisera<sup>†</sup> and James J. Valentini\*

Department of Chemistry, Columbia University, New York, New York 10027

Received: March 7, 1997; In Final Form: May 12, 1997<sup>⊗</sup>

We report a study of the reaction dynamics of the  $\text{H} + \text{CDCl}_3 \rightarrow \text{HD}(v',j') + \text{CCl}_3$  reaction with the  $\text{CDCl}_3$  reactant prepared in the  $\nu_1$  C–D stretch  $v''=1$  excited state. Stimulated Raman excitation is used to prepare the  $\text{CDCl}_3(v''=1)$  reactant and coherent anti-Stokes Raman scattering is used to detect the  $\text{HD}(v',j')$  product, under effectively single-collision conditions at a relative energy of 1.6 eV. Even though the vibrational excitation energy of the reactant (0.28 eV) is small compared to the collision energy, which greatly exceeds the reaction barrier height, the vibrational excitation of the reactant increases the reaction cross section by a factor of  $1.66 \pm 0.15$ . Despite this, none of the energy added by the reactant vibrational excitation appears as HD product vibration or rotation. All of it goes into product translation and/or  $\text{CCl}_3$  internal energy.

## Introduction

For many years, chemical physicists have uncovered a great deal about the dynamics of atom + diatom reactions.<sup>1</sup> Because in nature most important reactions involve polyatomic molecules, there are now attempts to explore more complex systems—systems of real chemical complexity—involving atom + polyatom reactions having reaction coordinates that combine, at least formally, many reactant and product degrees of freedom.<sup>2–6</sup> However, the information gained from the many experiments on atom + diatom systems forms the framework for understanding atom + polyatom reactions. The dynamics of the atom + diatom systems also provide the benchmark against which to measure how much of the potential high dimensionality of the reactive motion actually is important.

Our own efforts to understand the variation of reaction dynamics with increasing dimensionality of the reactive motion, or more loosely how the dynamics vary with the structure of the polyatomic reactant, have focused on reactions with a specific type of kinematics and thermochemistry. These reactions involve light + light–heavy kinematics, with H atoms being abstracted by H atoms to form  $\text{H}_2$ , in reactions that are thermoneutral, or nearly so. The photolytically generated reactant H atoms possess large velocities and give collision energies that far exceed the minimum energy path reactive barrier heights, so that a large portion of the multidimensional potential energy surface can be explored.

Our experiments began with a study of the  $\text{H} + \text{CD}_4 \rightarrow \text{HD}(v',j') + \text{CD}_3$  reaction.<sup>2</sup> This reaction has the same thermochemistry and light + light–heavy kinematics as the previously studied  $\text{H} + \text{HCl}$  reaction, which serves as the atom + diatom benchmark in these state-to-state dynamics studies.<sup>7,8</sup> The  $\text{H}_2/\text{HD}$  products of the two reactions are similar in some ways. However, while the  $\text{H}_2$  products from all the atom + diatom  $\text{H} + \text{HX}$  ( $\text{X} = \text{Cl}, \text{Br}, \text{I}$ ) reactions exhibit negative correlations between product vibrational energy and rotational energies (as in fact do all other atom + diatom reactions), the  $\text{H} + \text{CD}_4$  reaction yields products with a *positive* ( $v'-j'$ ) correlation. Further experiments demonstrated that this unusual positive correlation exists in the  $\text{H}_2$  product of the  $\text{H} + \text{C}_2\text{H}_6$  and  $\text{H} + \text{C}_3\text{H}_8$  reactions as well and gets stronger as the size of the alkane increases.<sup>3</sup>

This anomalous result, associated with the increased dimensionality of these polyatomic reactants and the multiplicity of identical reaction sites, indicates that a descriptive dynamics based on an atom + diatom picture would not suffice for these systems. It also indicated to us the necessity for stepping back to a simpler system, one with a reactive motion that was effectively of reduced dimensionality, that is, involving fewer modes of reactants and products, compared to that for the alkane reactions, yet similar to them energetically and structurally. The system we chose was the  $\text{H} + \text{CDCl}_3 \rightarrow \text{HD} + \text{CCl}_3$  reaction.<sup>9</sup>

The dynamics of this reaction should have a reactive motion that is of lower effective dimensionality, and hence more closely resemble the dynamics of the atom + diatom reactions, for two reasons. First, because the mass of the Cl atoms is quite large relative to the H and D masses, the motion of the Cl atoms should be largely decoupled from the motions of the H and D. Second, the pyramidal geometry of the  $\text{CCl}_3$  fragment is very close to that it has in the  $\text{CDCl}_3$  reactant, removing the potential energy gradient along the  $\text{CX}_3$  umbrella mode that exists in the  $\text{H} + \text{CD}_4$  reaction. Indeed, the dynamics of this reaction do fall between those of the  $\text{H} + \text{alkane}$  reactions and those of the  $\text{H} + \text{hydrogen halide}$  reactions, showing neither a positive ( $v'-j'$ ) correlation nor a negative one.

These observations invite considerable speculation, but no simple, conclusive interpretation. Given the potential complexity of the reactions, which seems to be realized, and their distinctive, even surprising, dynamical behavior, one might expect that more than these relatively few observations would be required to produce enough knowledge with which to build a convincing interpretation.

The experiments reported here aim to provide some of that knowledge by examination of the dynamics of these reactions from vibrationally excited states of the polyatomic reactant. The transition state couples vibrational modes of reactants with those of products, so reactions initiated with  $v''>0$  enable more detailed probing of the transition state than is possible with reactions from the vibrationless ground state. This is particularly true for these thermoneutral (or nearly thermoneutral) H-atom-abstraction-by-H-atoms reactions. These reactions invariably show very little coupling of the translation of the reactants with the internal modes of the products, even at high collision energy.

There has been long-standing interest in the reactions of vibrationally excited molecules. The question of the relative efficacy of vibrational energy in promoting a reaction at energies near threshold has been addressed by preparing reactants in

<sup>†</sup> Present address: Department of Chemistry, University of Virginia, Charlottesville, VA 22901.

<sup>⊗</sup> Abstract published in *Advance ACS Abstracts*, July 15, 1997.

specific vibrational states and observing the effect on the kinetic rate constants.<sup>10–12</sup> More recently there has been keen interest in mode-selective reactivity driven by vibrational excitation.<sup>13</sup> However, our interest is not in those questions. Rather, we wish to know how the specific energy present in the reactants is partitioned into the product quantum states, as a way to visualize the reaction coordinate in these many-dimensional  $\text{H} + \text{alkane}$  (substituted alkane) systems, an effort that is also underway for the  $\text{Cl} + \text{alkane}$  reactions.<sup>14</sup>

An unusually well informed reader will note something that distinguishes these two systems, though. For the  $\text{Cl} + \text{alkane}$  reactions the collision energies are not large compared to the reaction barrier heights, due to the heavy + light–heavy kinematics and the relatively low energies of the  $\text{Cl}$  atoms generated by  $\text{Cl}_2$  photolysis, so the effect of vibrational excitation, which exceeds the collision energy, is relatively easy to anticipate. For the  $\text{H} + \text{alkane}$  (substituted alkane) reactions we are studying, however, the vibrational excitation energy is substantially less than the collision energy, which already exceeds the minimum energy path barrier height. The reader who is both well informed and skeptical may be asking whether vibrational excitation of the reactant could make any difference at all in such circumstances. It can and does, and a lot of difference.

This is evident in a comparison of the dynamics of the far simpler  $\text{H} + \text{D}_2(\nu''=1) \rightarrow \text{HD}(\nu',j') + \text{D}^{15}$  and  $\text{D} + \text{H}_2(\nu''=1) \rightarrow \text{HD}(\nu',j')^{16} + \text{H}$  reactions. Even though the 1.3–1.4 eV collision energy is much greater than either the barrier height or the vibrational excitation energy, vibrational excitation of the reactant diatom very strongly affects the state-to-state dynamics. While the reactions show nearly indistinguishable dynamics for  $\nu''=0$  reactants, vibrational excitation differentiates them dramatically, such that they do not even appear to be taking place on the same potential energy surface. The differences result from the slightly different vibrationally adiabatic energetics of the two systems, differences which though small are magnified in the state-to-state cross sections of the  $\nu''=1$  reactions.<sup>15,17</sup>

## Experiment

The experimental apparatus used here is essentially identical to that used for our studies of the  $\text{H} + \text{D}_2(\nu''=1) \rightarrow \text{HD}(\nu',j') + \text{D}$  reaction.<sup>15</sup> With stimulated Raman excitation (SRE) we prepare the vibrationally excited  $\text{CDCl}_3$ , and with coherent anti-Stokes Raman scattering (CARS) we detect the  $\text{HD}(\nu',j')$  product. Photolysis of  $\text{HI}$  at 266 nm generates the  $\text{H}$  atom reactant.

All five of the required laser beams (two for SRE, two for CARS, and the single photolysis beam) originate from a single 10 Hz Q-switched, injection-seeded Nd:YAG laser (Continuum NY81-C-10). The 1064 nm fundamental is frequency-doubled to produce 530–540 mJ of 532 nm light. This beam operates with a spectral bandwidth of  $0.0045 \text{ cm}^{-1}$  and a temporal width of 6 ns fwhm. This 532 nm beam is split repeatedly to yield the four beams needed for SRE preparation of vibrationally excited  $\text{CDCl}_3$  reactant and CARS detection of the  $\text{HD}$  product. The 1064 nm light from the Nd:YAG that remains after the first doubling is itself doubled in frequency to produce 80 mJ of 532 nm light in a second beam. This second 532 nm beam is used to generate the 266 nm photolysis beam.

The vibrationally excited  $\text{CDCl}_3$  is prepared in the  $(\nu_1, \nu''=1)$  quantum state. The  $\nu_1$  vibration is the C–D stretch at  $2265 \text{ cm}^{-1}$ . The SRE process requires two beams, referred to as the “pump” and “Stokes”, respectively, whose frequency difference matches the  $2265 \text{ cm}^{-1} \nu_1 \nu=0 \rightarrow \nu=1$  transition frequency.

The SRE pump is a 75 mJ pulse at 532 nm, while the SRE Stokes is a 55 mJ pulse produced by a dye laser (Spectra-Physics PDL-2) operating at 604.9 nm with a fwhm linewidth of  $\sim 0.25 \text{ cm}^{-1}$ . Because of the congested Q-branch ground state spectrum of  $\text{CDCl}_3$ , most of the ground rotational levels can be accessed with the  $0.25 \text{ cm}^{-1}$  SRE excitation bandwidth.

Some of the 532 nm beam from the Nd:YAG laser pumps a second dye laser (Lumonics HD-500), which gives the tunable Stokes beam for the CARS process. This dye laser yields pulses of 10 to 15 mJ with a linewidth of  $0.06\text{--}0.08 \text{ cm}^{-1}$ . The remaining 532 nm light, approximately 30 mJ per pulse, provides the CARS pump beam. The last part of the 532 nm second harmonic of the Nd:YAG laser is frequency-doubled to produce  $\sim 10$  mJ of the 266 nm photolysis light.

The photolysis beam, the SRE beams, and the CARS beams are precisely overlapped spatially, so as to make them coincident within about  $20 \mu\text{m}$  at their common focus and collinear within about  $500 \mu\text{rad}$ . The photolysis, SRE, and CARS beams must pass through many optical components to achieve this alignment and overlap. Because of cumulative losses at these optical components, particularly losses at the dichroic and polarization-sensitive beam combining optics that make all four of these beams collinear and overlapped, the pulse energies delivered to the sample are much smaller than the nominal values quoted here. The optical layout of the experiment does not allow accurate measurement of the pulse energies actually incident on the sample, but these are one-half to one-tenth the nominal values.

Preparation of reactants in  $\nu''=1$  is the first step in the temporal sequence of the experiments. Initiation of reaction via  $\text{HI}$  photodissociation proceeds 4 ns after SRE. The CARS probe pulses arrive at the reaction region 10 ns after photolysis. An adjustable delay line makes variation in the relative timing of the CARS pulses convenient without altering the alignment of the beams. Vibrational relaxation of the  $\text{CDCl}_3$  in  $\nu''=1$  prior to reaction with the  $\text{H}$  atoms seems unlikely and is not observed. The probability of a collision of the  $\text{CDCl}_3$  in  $\nu''=1$  prior to  $\text{HD}$  product detection is very small, and collisionless intramolecular energy transfer seems also improbable, given the fact that all the other vibrational modes in  $\text{CDCl}_3$  have frequencies that are far removed from the  $2265 \text{ cm}^{-1}$  frequency of the  $\nu_1$ . These other vibrations occur at 914, 745, 655, 365, and  $259 \text{ cm}^{-1}$ . More compelling in this regard are our actual measurements that show no vibrational relaxation; CARS spectra of  $\text{CDCl}_3$  in  $\nu''=1$  at delays of 6 and 14 ns were identical.

In the experiments reagents are flowed into a  $0.6 \text{ cm}^3$  stainless steel reaction vessel suspended within the 6.7 L cell, as has been described previously.<sup>9</sup> The ends of the cell are closed by quartz windows, upon which argon buffer gas is flowed. The reaction vessel is open on both ends and in addition has one port for the introduction of both  $\text{HI}$  (Matheson Gas Products reaction grade, 98% purity) and  $\text{CDCl}_3$  (Cambridge Isotope Laboratories, 99.8% D), and two ports for vacuum pumping. The cell pressures of  $\text{HI}$ ,  $\text{CDCl}_3$ , and  $\text{Ar}$  in this experiment are 8, 2, and 10 Torr, respectively.

At the pressure and delay time used in this experiment, we are not quite in the single-collision domain. However, we studied the  $\text{H} + \text{CDCl}_3(\nu''=0)$  reaction under identical experimental conditions and found no evidence for any effects of multiple collisions. There was no discernible difference between the product distributions obtained under conditions identical to those used here and conditions that reduced all collision probabilities by one-half.<sup>9</sup> Therefore, we believe that the product distributions reported here represent those of single-collision conditions within stated uncertainties.

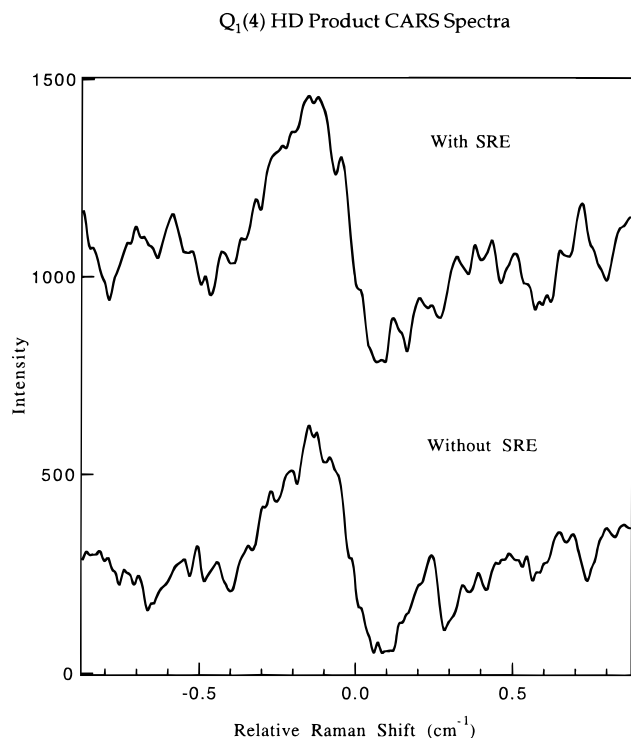


**Figure 1.** CARS spectra of HD( $v'=1, j'=4$ ) from the H + CDCl<sub>3</sub> reaction. The top spectrum is obtained with stimulated Raman excitation pumping 26% of the CDCl<sub>3</sub> to  $v''=1$ , while the bottom spectrum has all the reactant in  $v''=0$ .

Initiation of the reaction via photolysis of HI at 266 nm produces H atoms of two energies, 1.6 eV (66%) and 0.7 eV (34%).<sup>18</sup> The 1.6 eV H atoms contribute more to the HD product populations, but contributions from the 0.7 eV atoms cannot be neglected. If the reactive cross sections for the two collision energies were the same, the faster H atoms would produce 76% of the product. Because the potential energy surface for the H + CDCl<sub>3</sub> reaction is unknown, there is no direct method to determine the relative cross sections of this reaction at the two collision energies. However, classical trajectory calculations performed on the H + HX → H<sub>2</sub> + X (X = Cl, Br, I) reactions lead us to expect that  $\sigma_{1.6\text{eV}}/\sigma_{0.7\text{eV}}$  for H + CDCl<sub>3</sub> is 1 or greater and that the 0.7 eV collisions result in at most 25% of the HD product.<sup>8,9</sup> Although this contribution is small, it is not negligible and may affect the product distributions somewhat. However, the same ambiguity exists in the other light + light-heavy → light-light + heavy reactions studied thus far, including the H + CDCl<sub>3</sub>( $v''=0$ ) reaction. Comparisons of this experiment to other experiments having the same ambiguity should not be particularly troublesome.

### Spectra and Data Analysis

CARS scans over the various Q<sub>*v'*</sub>(*j'*) HD product transitions were taken with and without SRE to determine the HD( $v', j'$ ) populations and absolute partial cross sections. Two such scans, for the Q<sub>1</sub>(4) HD product, are shown in Figure 1. These spectra are presented here for illustrative purposes only. As is the case with such CARS spectra, the dependence on product number density difference rather than number density itself, the nonlinear nature of this density difference dependence, and the complicated line-shape function do not allow a simple visual assessment of the product yields from the spectral peak heights. Quantitative analysis requires consideration of the complete functional dependence of the CARS signal on species density, which is described below.

At least 16 scans were recorded, eight with SRE and eight without SRE, for each reported transition, so as to improve the quality of the quantum state distributions and absolute partial cross sections. In addition, CARS reference scans were taken to correct for drifts in the CARS detection system and the SRE reactant state preparation system. Periodic scans of the relatively strong HD Q<sub>0</sub>(5) product transition were taken without SRE to account for drifts in the CARS detection system. Any changes in this signal indicate a change in reactant density or photolysis efficiency, changes in the Stokes and pump CARS laser beams, or changes in other variables not connected with SRE preparation of reactants.

For this experiment, reference scans serve as a guide to the reliability of the data. Recording several scans helped reduce the influence of fluctuations among the various scans. The method of recording spectra for each nonreference Q-branch transition is also designed to minimize the effect of any linear drift in the system that does occur. First, we record a scan with SRE, then continue with two scans without SRE, followed by two more scans with SRE, two without SRE, and a final scan with SRE. For each transition recorded in this experiment, at least two such sequences were performed on separate days, allowing for more reliable data acquisition and minimization of systematic errors.

The second type of reference scan, not necessary in the H + CDCl<sub>3</sub>( $v''=0$ ) reaction, involves determining the SRE efficiency at regular intervals. We do this by taking CARS spectra of the reactant CDCl<sub>3</sub> Q-branch transition with and without stimulated Raman excitation. An example of such a scan pair is given in Figure 2. Such spectra are possible because the dye used in the CARS Stokes laser has output in the wavelength ranges needed to probe both CDCl<sub>3</sub> and HD. Because of the large moments of inertia of the CDCl<sub>3</sub> molecule, virtually all of the rotational Q-branch lines appear within the 0.25 cm<sup>-1</sup> bandwidth of the SRE convolution. We performed CARS scans of CDCl<sub>3</sub> reactant at various intervals throughout the experiment and were able to determine the percent of population transfer to within less than ±1%. Over the course of the experiment, these observed SRE efficiencies, that is, population transfers to  $v''=1$ , were in the range 18–28% of the total CDCl<sub>3</sub>.

The magnitude of a CARS signal is given by

$$S(\omega_{\text{as}}) = B \int g(\omega; \omega_{\text{as}}) F_2 |\chi^{(3)}|^2 d\omega \quad (1)$$

where  $B$  is a constant proportional to  $I_p^2 I_s$  and  $g(\omega; \omega_{\text{as}})$  is the CARS laser line-shape function, centered at  $\omega_{\text{as}}$ .  $F_2$  is a term related to focusing and is given by<sup>19</sup>

$$F_2 = 4\pi^2 \omega_{\text{as}}^4 \left[ 1 + \frac{(2\omega_p + \omega_s)^2}{(2\omega_p - \omega_s)^2} \right] \quad (2)$$

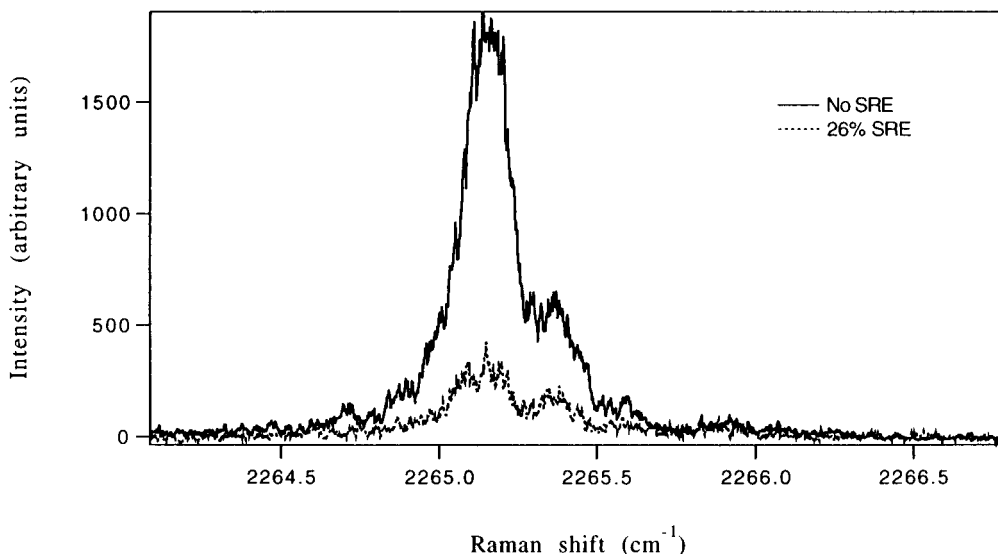
The third-order nonlinear susceptibility term,  $\chi^{(3)}$ , consists of three components,

$$\chi^{(3)} = \chi' + i\chi'' + \chi^{\text{NR}} \quad (3)$$

where  $\chi'$  and  $\chi''$  are the real and imaginary frequency-dependent Raman resonance terms of the susceptibility, and  $\chi^{\text{NR}}$  is the frequency-independent nonresonant susceptibility. According to eq 1, then,

$$S(\omega_{\text{as}}) \propto (\chi')^2 + (\chi'')^2 + (\chi^{\text{NR}})^2 + 2\chi'\chi^{\text{NR}} \quad (4)$$

Both  $\chi'$  and  $\chi''$  are directly proportional to  $\Delta N$ , the population difference between the ( $v', j'$ ) and ( $v'+1, j'$ ) quantum states

CARS Spectra of  $\text{CDCl}_3$  Q-branch with and without SRE

**Figure 2.** Representative CARS reference spectra of the  $\text{CDCl}_3$   $Q_0(J,K)$ -branch with and without SRE. The scan taken without SRE has an intensity 4.3 times that in the scan with SRE, indicating 26% population transfer to  $v''=1$ .

connected by the Raman transition and are dependent on the frequency, linewidth, and Raman cross section of the transition.

For the HD reaction product,  $\chi'$  and  $\chi''$  are both quite a bit smaller than  $\chi^{\text{NR}}$ , so the  $(\chi^{\text{NR}})^2$  and  $2\chi'\chi^{\text{NR}}$  terms in eq 4 dominate. Because  $\chi'$  is dispersive about the Raman resonance frequency, the CARS spectra also have a largely dispersive form in the region of the Raman resonance, as shown in Figure 1. By contrast,  $\chi'$  and  $\chi''$  are much larger than  $\chi^{\text{NR}}$  for the  $\text{CDCl}_3$  reactant, as illustrated in Figure 2, so the  $(\chi')^2$  and  $(\chi'')^2$  terms dominate the CARS signal, and this signal then depends directly on  $(\Delta N)^2$ , making analysis of the CARS spectra to determine  $\Delta N$  for the reactant very simple and very accurate.

Analysis of CARS spectra in which  $\chi'$  and  $\chi''$  are comparable to or smaller than  $\chi^{\text{NR}}$  is algebraically complicated, because the signal depends on the interplay of the  $(\chi^{\text{NR}})^2$  and  $2\chi'\chi^{\text{NR}}$  terms in eq 4 and thus in a complicated way on  $\Delta N$ , the laser linewidth, the focusing of the CARS beams, and other factors. In our previous CARS experiments, including the  $\text{H} + \text{CDCl}_3(v''=0)$  experiment,<sup>9</sup>  $\Delta N$  was determined by using eq 1 to calculate ResSig/BackSig, the ratio of the resonant CARS signal (ResSig) at the vibrational Q-branch resonance frequency to the nonresonant background signal (BackSig), as a function of  $\Delta N$  for the particular experimental conditions. For dispersive spectra, ResSig is the difference between the  $S(\omega_{\text{as}})$  maximum (above the nonresonant background value of  $S(\omega_{\text{as}})$ ) and the  $S(\omega_{\text{as}})$  minimum (below the nonresonant background value of  $S(\omega_{\text{as}})$ ). The experimental value of  $\Delta N$  is taken as the value of  $\Delta N$  in the calculation that reproduces the experimental ResSig/BackSig ratio.

With this method only a small fraction of the several hundred data points per scan are actually used to determine  $\Delta N$ . A fitting method that uses all of the experimentally obtained data improved this analysis markedly for the  $\text{H} + \text{D}_2(v''=1)$  experiment.<sup>15</sup> For this procedure, the entire scan was fitted to a calculated line shape to extract the correct value of  $\Delta N$ .

For the  $\text{H} + \text{CDCl}_3(v''=1)$  experiment, however, such a fitting program became problematic. For some scans the least-squares fitting procedure became sensitive to fluctuations in the spectrum at frequencies away from the Raman resonance, where the signal-to-noise ratio was low, causing convergence problems. Also, for this system with diatom + polyatom products, the

translational energy of the products, which determines the product transition linewidth, is not automatically specified by energy conservation for each  $\text{HD}(v',j')$  product, so the transition linewidth must be incorporated as an additional parameter in the fit.

For our earlier  $\text{H} + \text{D}_2$  and  $\text{H} + \text{HX}$  reaction studies, the translational energy of the HD or  $\text{H}_2$  product in a specific  $(v',j')$  quantum state is known with certainty without measurement as a consequence of conservation of energy, knowledge of the total available energy, and specification of the product internal energy via determination of  $v'$  and  $j'$ . However, for  $\text{H} + \text{RD}$  reactions in which RD is a polyatom, the HD product translational energy must be measured. This translational energy can be determined from the HD CARS spectrum using a variable transition linewidth in the CARS fitting procedure. However, obtaining reliable transition linewidths from modest signal-to-noise-ratio spectra is not easy.

So, instead of simultaneously extracting the transition linewidth and population from each HD product CARS spectrum, a method of determining ResSig/BackSig that was insensitive to transition linewidth was devised. This method is analogous to determining the strength of a Gaussian or Lorentzian line shape by summation of all the data points minus the background level. However, for a dispersive CARS signal, such a summation is not appropriate. Rather, it is the *absolute value* of the deviation from the background which is indicative of signal strength. Because ResSig is fundamentally a measure of the deviation from the background, the sum of the absolute values of the difference between the signal and background over 200 points about the Raman resonance is linearly proportional to ResSig. Previously, a determination of maximum and minimum values of the dispersive signal using only  $\sim 50$  points sufficed for the determination of  $\Delta N$ . The use of more data points in the analysis done here increased the precision and accuracy of the measurements and allowed for the determination of the populations given in the following section.

Analysis of CARS spectra yields only the difference in population between the  $(v',j')$  level and the  $(v'+1,j')$  level connected by the CARS transition. Therefore, determination of the population of a  $(v',j')$  level requires knowledge of the population of the  $(v'+1,j')$  level. The population of a given

$(v', j')$  level is given by

$$N(v', j') = \sum_{v''=v'}^{v''=2} \Delta N(v', j') \quad (5)$$

because no population in  $v' \geq 3$  was observed. Some  $(v', j')$  populations were not measured, so we determined populations for  $(v'-1, j')$  in these cases by adding the experimentally determined difference in population between the  $(v'-1, j')$  level and the  $(v', j')$  level to an estimate of the population of the  $(v', j')$  level. These estimates are calculated via a best fit linear surprisal analysis to the measured  $(v', j')$  populations.

Since we compare here the  $\text{H} + \text{CDCl}_3(v''=0) \rightarrow \text{HD}(v', j') + \text{CCl}_3$  and  $\text{H} + \text{CDCl}_3(v''=1) \rightarrow \text{HD}(v', j') + \text{CCl}_3$  reactions, it is most convenient and appropriate to determine the partial cross sections for the  $\text{CDCl}_3(v''=1)$  reaction relative to the partial cross sections for the HD product of the  $\text{H} + \text{CDCl}_3(v''=0)$  reaction. This requires only a comparison of the product populations extracted from the with SRE and without SRE spectra, obtained in the same experiment at the same time, as described above, and a knowledge of the amount of  $v''=1$  reactant population with SRE. The uncertainty in the determination of the latter (better than  $\pm 1\%$  out of 23%) is small enough that it makes little contribution to the uncertainty in the determination of the relative cross sections. These relative cross sections can be converted to absolute cross sections since we have previously measured the absolute cross sections for the  $\text{H} + \text{CDCl}_3(v''=0)$  reaction to be  $0.55 \pm 0.10 \text{ \AA}^2$ .<sup>9</sup>

## Results and Discussion

The principal observables in these experiments are the individual partial cross sections for all the product  $\text{HD}(v', j')$  states of the  $\text{H} + \text{CDCl}_3(v''=1)$  reaction. These are given as absolute partial cross sections for each measured HD rovibrational product state in Table 1, along with corresponding data for the  $\text{H} + \text{CDCl}_3(v''=0)$  reaction. The uncertainties quoted are due to uncertainties in the measured product CARS spectra, uncertainties in the  $v''=1$  reactant population, and the uncertainty in the absolute cross section of the  $v''=0$  reaction, which are accounted for using standard statistical approaches.<sup>20</sup>

While some  $v', j'$  states could not be accurately measured, and cross sections for them are not given in Table 1, there are enough observed product quantum states, representing about 70% of all products, to determine with reliability the energy partitioning and surprisal parameters.<sup>9,15</sup> The total reaction cross section of the  $\text{H} + \text{CDCl}_3(v''=1) \rightarrow \text{HD} + \text{CCl}_3$  reaction, summed over  $v'$  and  $j'$  (using the surprisal analysis to estimate the contributions from those  $v', j'$  states not directly observed) is  $0.92 \pm 0.26 \text{ \AA}^2$ .

The uncertainty in this absolute cross section has its largest contribution from the uncertainty in the absolute cross section of the  $v''=0$  reaction to which it is referenced. The magnitude of the  $\text{H} + \text{CDCl}_3(v''=1) \rightarrow \text{HD} + \text{CCl}_3$  cross section relative to that for the  $\text{H} + \text{CDCl}_3(v''=0) \rightarrow \text{HD} + \text{CCl}_3$  ground vibrational state reaction is much better established in our experiments. The relative yields of HD with and without vibrational excitation of the reactant do not require knowledge of or measurement of as many experimental quantities and thus have smaller errors. We find that, summed over all  $v'$  and  $j'$ , the ratio  $\sigma(v''=1)/\sigma(v''=0) = 1.66 \pm 0.15$ .

Aside from this overall increase in total product yield, the product partial cross sections for the  $\text{H} + \text{CDCl}_3(v''=1) \rightarrow \text{HD}(v', j') + \text{CCl}_3$  reaction are quite similar to those for the  $\text{CDCl}_3(v''=0)$  reaction. Table 1 and Figure 3 show that for HD product in  $v''=0$  there is an increase in cross sections for most

**TABLE 1: Absolute Partial Cross Sections for the  $\text{H} + \text{CDCl}_3(v''=0,1) \rightarrow \text{HD}(v', j') + \text{CCl}_3$  Reactions**

quantum state ( $v', j'$ )	$\sigma (\text{\AA}^2)$	
	$v''=1$	$v''=0^a$
(0,0)		0.020(3) <sup>b</sup>
(0,1)		0.032(4)
(0,2)	0.070(13)	0.033(4)
(0,3)	0.084(32)	0.038(3)
(0,4)	0.082(20)	0.045(4)
(0,5)	0.127(18)	0.044(3)
(0,6)	0.040(13)	0.039(4)
(0,7)		0.031(4)
(0,8)		
(0,9)	0.035(11)	0.028(3)
(0,10)	0.035(11)	0.022(3)
(0,11)	0.016(11)	0.017(4)
(0,12)	0.022(8)	0.015(3)
(1,2)	0.0088(35)	0.0102(12)
(1,3)		0.0101(9)
(1,4)	0.0152(60)	0.0114(11)
(1,5)	0.0325(58)	0.0138(12)
(1,6)	0.0197(63)	0.0112(21)
(1,7)		0.0107(15)
(1,8)	0.0119(46)	
(1,9)		0.0087(12)
(1,10)	0.0115(36)	
(2,1)	0.0050(11)	0.0030(5)
(2,2)		0.0032(4)
(2,3)	0.0030(20)	0.0030(5)
(2,4)	0.0022(14)	0.0044(6)
(2,5)		0.0049(6)
(2,6)	0.0064(14)	0.0038(10)
(2,7)	0.0061(28)	0.0029(5)

<sup>a</sup> Data from ref 9. <sup>b</sup> Numbers in parentheses represent uncertainties in the least significant digit(s).

HD rovibrational states, but such changes are not  $j'$  specific. The average  $v''=0$  product rotational quantum number  $\langle j' \rangle$  changes immeasurably from 5.6 to 5.5, but the total reactive cross section into  $v''=0$  does increase by a factor of 1.6.  $\text{CDCl}_3$  vibrational excitation enhances reactive channels leading to HD population in  $v''=0$ , but such an enhancement is independent of rotational state.

A plot similar to Figure 3 for HD in  $v''=1$  is given in Figure 4. The  $v''=1$  data in this figure and in Table 1 indicate perhaps a weak change in the product rotational distribution upon vibrational excitation of the  $\text{CDCl}_3$  reactant. Similar to what is observed for  $v''=0$ , the total cross section for  $v''=1$  increases by a factor of 1.6, but instead of remaining the same, as is the case in  $v''=0$ , here  $\langle j' \rangle$  increases from 5.6 to 6.8 upon  $\text{CDCl}_3$  vibrational excitation.

Data for HD  $v''=2$  involve large uncertainties and measurement for only five  $j'$  quantum states, making any conclusions about the rotational distributions unreliable. However, using a linear surprisal analysis of the  $(v''=2, j')$  rotational state distribution, one can estimate the increase in the total  $v''=2$  cross section upon vibrational excitation of the  $\text{CDCl}_3$  to be a factor of 1.7. Therefore, the increase in cross section is virtually the same for all vibrational levels. Because of this, the  $\text{HD}(v')$  distribution is virtually unchanged between  $v''=0$  and  $v''=1$  reactants. Upon  $\text{CDCl}_3$  reactant vibrational excitation,  $\langle v' \rangle$  for the HD product increases insignificantly from 0.31 to 0.32. The detailed product vibrational state distributions for the  $v''=1$  and  $v''=0$  reactions are compared in Figure 5. The absolute cross sections into  $v''=0, 1$ , and 2 are 0.68(6), 0.18(2), and 0.06(1)  $\text{\AA}^2$ , respectively, for  $v''=1$ , while the corresponding cross sections for  $v''=0$  reactant are 0.41(1), 0.11(1), and 0.033(4)  $\text{\AA}^2$ .

A comparison of the energy partitioning in the  $\text{CDCl}_3(v''=1)$  and  $\text{CDCl}_3(v''=0)$  reactions is given in Table 2. For both

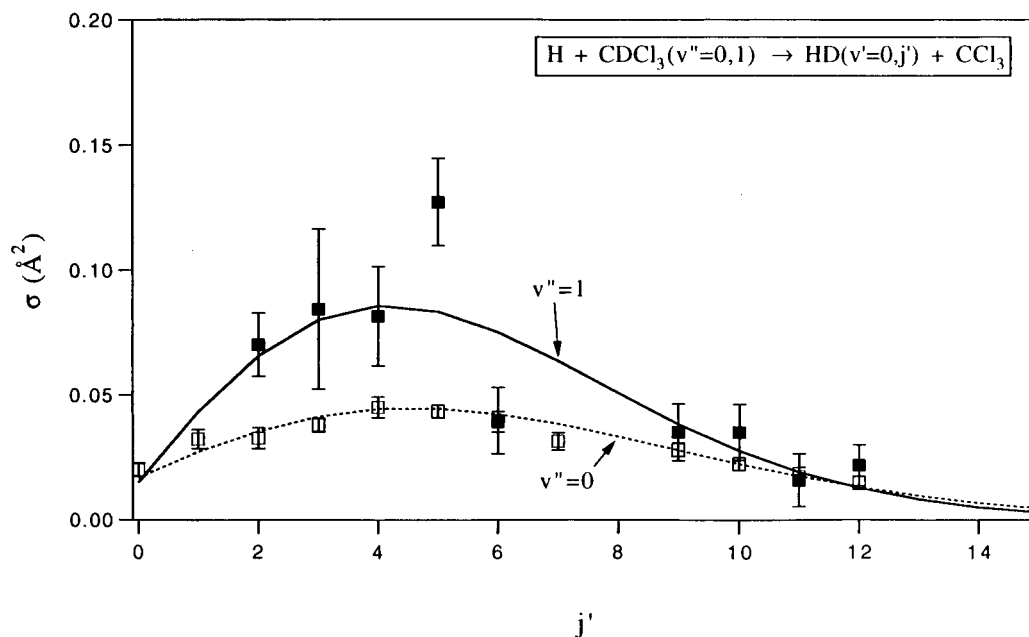


**Figure 3.**  $\text{HD}(\nu'=0,j')$  partial cross sections for the  $\text{H} + \text{CDCl}_3(\nu''=0,1)$  reactions plotted versus the rotational quantum number,  $j'$ . The solid squares show data for  $\nu''=1$ , and the open squares are data for  $\nu''=0$ . Error bars represent  $\pm 1$  standard deviation. The solid and dashed lines are linear surprisal fits for the  $\nu''=1$  and  $\nu''=0$  data, respectively, and are characterized by  $\Theta_r = 8.7$  and  $6.4$ , with the  $\text{CCl}_3$  treated as an atom.

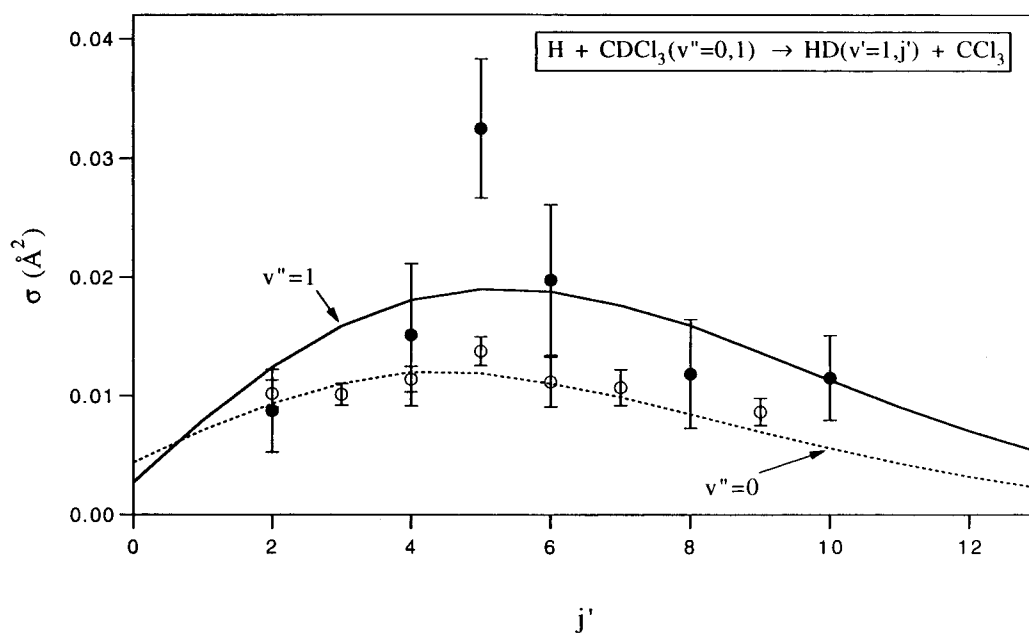


**Figure 4.**  $\text{HD}(\nu'=1,j')$  partial cross sections for the  $\text{H} + \text{CDCl}_3(\nu''=0,1)$  reactions plotted versus the rotational quantum number,  $j'$ . The solid circles show data for  $\nu''=1$ , and the open circles are data for  $\nu''=0$ . Error bars represent  $\pm 1$  standard deviation. The solid and dashed lines are linear surprisal fits for the  $\nu''=1$  and  $\nu''=0$  data, respectively, and are characterized by  $\Theta_r = 4.5$  and  $4.4$ , with the  $\text{CCl}_3$  treated as an atom.

reactions less than half of the reactant energy appears as HD product internal energy, with vibrational excitation the least important energy repository. However, within experimental error, none of the additional reactant energy represented by the  $\nu_1$   $\nu''=1$  reactant vibrational excitation appears as HD product rotation or vibration. And, because this excitation raises the total available energy, the fraction of energy in HD product vibration and rotation actually decreases. Although we have not determined it by direct experimental measurement, this means that both the amount of energy and the fraction of the available energy appearing in product translation plus  $\text{CCl}_3$  internal energy increase for the  $\nu''=1$  reaction.

It would be more than helpful to know the amount of energy contained in internal degrees of freedom of the  $\text{CCl}_3$  radical. However, the spectroscopy of  $\text{CCl}_3$  is not well enough charac-

terized to permit direct determination of its internal energy. In addition, the signal-to-noise ratios in the  $\text{HD}(\nu',j')$  Q-branch spectra are too low to permit direct determination of the translational recoil energy from the CARS line shape at the current spectroscopic resolution, as discussed above. In the HD product spectra, both with and without SRE, the transition linewidths that best fit the data are less than those that would be observed if there were no energy in the  $\text{CCl}_3$  product. However, because of the present inability to fit the line shapes with great accuracy and the low signal-to-noise ratios present in the experiment, the actual amount of translational energy in the HD products has not been determined. As a result, the partitioning between  $\text{CCl}_3$  internal energy and product translational energy remains unresolved.

Most of the 0.41 eV of HD internal energy appears as rotation

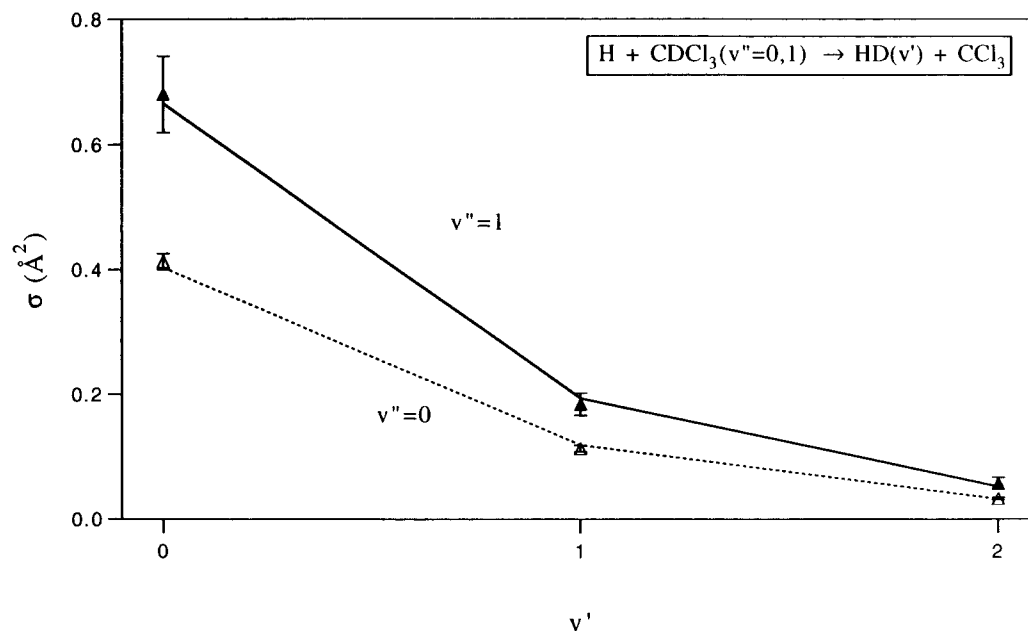


**Figure 5.** HD( $v'$ ) partial cross sections for the H + CDCl<sub>3</sub>( $v''=0,1$ ) reactions. The solid triangles show data for  $v''=1$ , and the open triangles are data for  $v''=0$ . Error bars represent  $\pm 1$  standard deviation. The solid and dashed lines are linear surprisal fits for the  $v''=1$  and  $v''=0$  data, respectively, and are characterized by  $\lambda v = 3.5$  and  $4.6$ , with the CCl<sub>3</sub> treated as an atom.

**TABLE 2: Energy Partitioning in the H + CDCl<sub>3</sub>( $v''=0,1$ )  $\rightarrow$  HD( $v',j'$ ) + CCl<sub>3</sub> Reactions**

quantity	$v''=0^a$	$v''=1$	difference
$E_{\text{avl}}$ (eV)	1.9	2.2	0.28
$\langle E_r \rangle$ (eV)	0.14	0.14	0.00
$\langle E_v \rangle$ (eV)	0.28	0.27	-0.01
$v'=0$	0.28	0.24	-0.04
$v'=1$	0.28	0.33	+0.05
$f_v$	0.07	0.07	0.00
$f_r$	0.15	0.12	-0.03

<sup>a</sup> Data from ref 9.

(0.27 eV), but the changes from the  $v''=0$  reaction are insignificant. Interestingly, the average rotational energy for  $v'=0$  decreases slightly, while the average rotational energy for  $v'=1$  increases slightly. Such a positive correlation between rotational and vibrational energy exists in the HD and H<sub>2</sub> product of the  $v''=0$  reactions of H + CD<sub>4</sub>, H + C<sub>2</sub>H<sub>6</sub>, and H + C<sub>3</sub>H<sub>8</sub>, but the HD product from the H + CDCl<sub>3</sub>( $v''=0$ ) reaction shows no correlation. The average vibrational energy in the HD product does not change upon CDCl<sub>3</sub> vibrational excitation despite the adiabatic exoergic of the reaction. There is no selective channeling of reactant vibration into product vibration at all. By contrast, the adiabatically endoergic H + D<sub>2</sub>( $v''=1$ ) reaction exhibits a small, but definite, increase in vibrational excitation of HD upon reactant excitation,<sup>15</sup> and the adiabatically exoergic D + H<sub>2</sub>( $v''=1$ ) reaction shows a strong propensity to produce vibrationally excited product HD.<sup>16</sup>

Vibrational excitation of the CDCl<sub>3</sub> reactant in the H + CDCl<sub>3</sub> reaction adds 0.28 eV to the initial energy. While this energy is a significant amount, it is smaller than the 0.36 eV exothermicity of the reaction and much smaller than the 1.6 eV collision energy that is already well above the reaction barrier. Yet, the addition of this vibrational energy does increase the reactive cross section, by a factor of  $1.66 \pm 0.15$ , an amount that while hardly dramatic, is still significant. This increase implies that the C–D stretch coordinate is an important component of the reaction coordinate even at high collision energy.

This makes the absence of any selective enhancement of any particular HD product rotational or vibrational states and the

failure of any of the additional reactant energy to appear as rotation or vibration of the HD product surprising by contrast. Large curvature in the reaction path after the reaction barrier is surmounted could mix the degrees of freedom that are parallel and perpendicular at the saddle point. Such mixing could dissipate what was initially the C–D stretch vibrational energy so that it would be distributed over the many degrees of freedom of the products. Since the density of states of the CCl<sub>3</sub> radical are so high, while the HD density of states is so low, much or all of the energy could appear as internal energy of the radical. However, this seems dynamically unlikely, given the disparity in the time scales of the motions of the light H,D atoms and the heavy Cl atoms and is at odds with the observed energy disposal in the H + CDCl<sub>3</sub>( $v''=0$ )  $\rightarrow$  HD( $v',j'$ ) + CCl<sub>3</sub> reaction.

The C–D stretch vibration is perpendicular to the reaction coordinate in the asymptotic reactant valley, so curvature of the reaction coordinate prior to the barrier crossing is needed to couple it to the reaction coordinate. However, for the system to evolve so as to channel what was initially the C–D stretch vibrational energy largely into product translation, the reaction path curvature after the barrier crossing would have to be small. This too seems dynamically unlikely in this slightly exoergic reaction.

The answer to which of these (apparently unlikely) dynamical behaviors is the actual behavior depends on an actual measurement of the product recoil energy. In fact, a better understanding of all the H + polyatomic RH  $\rightarrow$  H<sub>2</sub> + R reactions we have studied so far rests on making such measurements. We are now attempting to provide just such information, using our new microscale time-of-flight velocity measurements.<sup>21</sup>

It would also be helpful to know how much of this behavior is a consequence of the polyatomic nature of the CDCl<sub>3</sub> reactant and how much is due simply to the thermochemistry of the H + CDCl<sub>3</sub>  $\rightarrow$  HD + CCl<sub>3</sub> reaction. The strong divergence of the dynamics of the H + D<sub>2</sub>( $v''=1$ )  $\rightarrow$  HD( $v',j'$ ) + D<sup>15</sup> and D + H<sub>2</sub>( $v''=1$ )  $\rightarrow$  HD( $v',j'$ ) + H<sup>16</sup> reactions, which are essentially indistinguishable for reaction from  $v''=0$ , tells us that our understanding of the dynamics of vibrationally excited reactants is poor, even for the simplest systems. For that reason, studies of the H + HCl( $v''=1$ )  $\rightarrow$  H<sub>2</sub>( $v',j'$ ) + Cl and H + HBr( $v''=1$ )

$\rightarrow \text{H}_2(v',j') + \text{Br}$  reactions, which have the same kinematics as the  $\text{H} + \text{CDCl}_3 \rightarrow \text{HD} + \text{CCl}_3$  reaction and thermochemistry that bracket its own, would be desirable and are planned.

**Acknowledgment.** This work is supported by the Division of Chemical Sciences, Office of Basic Energy Sciences, Office of Energy Research, U.S. Department of Energy.

### References and Notes

- (1) Bernstein, R. B.; Levine, R. D. *Molecular Reaction Dynamics and Chemical Reactivity*; Oxford University: London, 1987.
- (2) Germann, G. J.; Huh, Y. D.; Valentini, J. J. *Chem. Phys. Lett.* **1991**, *183*, 353. Germann, G. J.; Huh, Y. D.; Valentini, J. J. *J. Chem. Phys.* **1992**, *96*, 1957.
- (3) Germann, G. J.; Huh, Y.-D.; Valentini, J. J. *J. Chem. Phys.* **1992**, *96*, 5746.
- (4) Simpson, W. R.; Rakitzis, T. P.; Kandel, S. A.; Lev-On, T.; Zare, R. N. *J. Phys. Chem.* **1996**, *100*, 7938. Kandel, S. A.; Rakitzis, T. P.; Lev-On, T.; Zare, R. N. *J. Chem. Phys.* **1996**, *105*, 7550.
- (5) Varley, D. F.; Dadigian, P. J. *J. Phys. Chem.* **1995**, *99*, 9843. Varley, D. F.; Dadigian, P. J. *J. Phys. Chem.* **1996**, *100*, 4365.
- (6) Yen, Y.-F.; Wang, Z.; Xue, B.; Koplitz, B. *J. Phys. Chem.* **1994**, *98*, 4.

- (7) Aker, P. M.; Germann, G. J.; Valentini, J. J. *J. Chem. Phys.* **1989**, *90*, 4795.
- (8) Aker, P. M.; Valentini, J. J. *Isr. J. Chem.* **1990**, *30*, 157.
- (9) Lanzisera, D. V.; Valentini, J. J. *Chem. Phys. Lett.* **1993**, *216*, 122. Lanzisera, D. V.; Valentini, J. J. *J. Chem. Phys.* **1994**, *101*, 1165.
- (10) Kneba, M.; Wolfrum, J. *Annu. Rev. Phys. Chem.* **1980**, *31*, 47.
- (11) Smith, I. W. M. *Acc. Chem. Res.* **1990**, *23*, 101.
- (12) Rubahn, H.-G.; Bergmann, K. *Annu. Rev. Phys. Chem.* **1990**, *41*, 735.
- (13) Crim, F. F. *J. Phys. Chem.* **1996**, *100*, 12725.
- (14) Simpson, W. R.; Orr-Ewing, A. J.; Zare, R. N. *Chem. Phys. Lett.* **1993**, *212*, 163. Simpson, W. R.; Rakitzis, T. P.; Kandel, S. A.; Orr-Ewing, A. J.; Zare, R. N. *J. Chem. Phys.* **1995**, *103*, 7313. Kandel, S. A.; Rakitzis, T. P.; Lev-On, T.; Zare, R. N. *Chem. Phys. Lett.* **1997**, *265*, 121.
- (15) Lanzisera, D. V.; Valentini, J. J. *J. Chem. Phys.* **1995**, *103*, 607.
- (16) Adelman, D. E.; Shafer, N. E.; Kliner, D. A. V.; Zare, R. N. *J. Chem. Phys.* **1992**, *97*, 7323.
- (17) Murphy, R. K.; Bernacki, K.; Valentini, J. J. To be published.
- (18) Clear, R. D.; Riley, S. J.; Wilson, K. R. *J. Chem. Phys.* **1975**, *63*, 1340.
- (19) Bjorklund, G. E. *IEEE J. Quantum Electron.* **1975**, *11*, 287.
- (20) Bevington, P. R.; Robinson, D. K. *Data Reduction and Error Analysis for the Physical Sciences*; McGraw Hill: New York, 1992.
- (21) Ni, H.; Serafin, J. M.; Valentini, J. J. *J. Chem. Phys.* **1996**, *104*, 2259.